

Numerical investigation of axial-vertical and lateral-vertical pipeline/soil interaction in sand

N. Daiyan & S. Kenny
Memorial University, St. John's, NL, Canada
R. Phillips
C-CORE, St. John's, NL, Canada
R. Popescu
URS Corporation, Princeton, NJ, USA



ABSTRACT

This numerical study is focused on an improved understanding of complex soil failure processes and load transfer mechanisms during combined axial-vertical (upward) relative pipeline/soil displacement events associated with large ground deformation hazards in sand. A parametric study has been conducted using the continuum finite element method with the software package ABAQUS. A range of practical design parameters such as pipeline burial depth vs. diameter ratio, soil properties, pipeline/soil interface friction angle and relative angles of movements are investigated. The outcome of numerical investigations is compared with available data in literature. Interaction diagrams that characterize the coupled soil load-displacement mechanisms in oblique axial-vertical direction are developed and discussed. The interaction curves for axial-lateral and lateral-vertical pipeline/soil interactions are also reviewed. These interaction diagrams provide an engineering basis to develop alternative soil spring formulations that account for coupled soil deformation mechanisms during pipeline/soil relative movement.

RÉSUMÉ

C'est numérique étude ciblée sur une amélioration de compréhension des processus complexes et l'échec du sol permet de mécanismes de transfert Au cours de la axiale combinée à la verticale par rapport Pipeline / événements de déplacement du sol des dangers associés à la déformation grand terrain dans le sable. Une étude paramétrique effectuée à l'aide continuum a été la méthode des éléments finis avec le logiciel Abaqus. Une gamme de pratiques paramètres de conception comme je suis donc heureux ensouillage de pipe Profondeur rapport, les propriétés du sol, d'un pipeline / angle de frottement du sol interface et des mouvements relatifs des angles sont étudiés. Les résultats des enquêtes numériques sont comparées aux données disponibles dans la littérature. Diagrammes d'interaction que nous caractérisons la charge couplée sol-Mécanismes de déplacement axial oblique dans les pays développés et la direction verticale sont discutées. L'interaction entre les courbes pour la canalisation axiale, latérale et verticale-latérale / interactions sol sont examinées aussi. Ces diagrammes d'interaction Fournir une base d'ingénierie pour développer notre alternative formulations du sol au printemps que nous rendre compte de la déformation du sol couplé mécanismes Pendant le mouvement du sol Pipeline / relative.

1 INTRODUCTION

Geohazards like landslides are one of the major sources of failures in oil and gas pipelines. Large permanent ground deformations impose large loads to pipelines over part of their length. Depending on the direction of relative movement between pipeline and soil with respect to pipeline elongation, the stress and strain state at each section of pipe will change. Evaluating the amount of soil load or restraint on the pipeline is a major task in pipeline geotechnics and understanding this effect is important for pipeline designers.

Using structural models for pipe/soil interaction including beam and spring elements to represent pipeline and soil respectively is a practical approach that has served pipelines industry to date. In the current engineering guidelines (e.g. Honegger and Nyman 2004) soil behavior is evaluated using discrete springs with load-displacement relationships provided in three perpendicular directions (i.e. longitudinal, lateral horizontal and vertical).

These springs are independent and during a 3D pipe/soil relative displacement they can not account for cross effects between loads in these three perpendicular directions.

The general form of the load-displacement relationships used for soil springs can be expressed as:

$$T = f(x); \quad P = g(y); \quad Q = h(z) \quad [1]$$

where T , P and Q are soil loads applied to the unit length of the pipeline and x , y and z are relative displacements between pipe and soil in longitudinal, lateral (horizontal) and vertical directions respectively.

The force-displacement relationships during pipeline/soil interaction are nonlinear and can be defined by bilinear or hyperbolic functions, which are proposed in guidance documents for pipeline engineering (e.g. ALA 2001, Honegger and Nyman 2004) and from other

analogous systems such as pile engineering. Bilinear relationships are usually used for simplicity.

Unlike the simplifications used in engineering practice, the relative movement between pipelines and soil during a ground movement incident may occur in axial, lateral and vertical directions at the same time. For instance, it is rare to have pure axial pipe/soil relative displacement without any lateral or vertical displacements. While there are many studies in the literature, investigating the lateral-vertical pipe/soil interaction, there are a limited number of studies on axial-lateral pipe/soil interaction and there is almost no study on axial-vertical pipe/soil interaction.

Previous experimental and numerical studies by the authors (Daiyan et al. 2010a & 2010b) have shown the importance of cross effects between axial and lateral (horizontal) soil restraints on the pipeline during oblique axial-lateral pipeline/soil relative movements. That analysis showed for a range of oblique angles the axial soil restraint on the pipeline increases as a result of increase in normal stresses on the pipeline/soil interface due to lateral movement of pipe in the soil media.

This paper investigates the axial-vertical pipe/soil interaction. The same continuum finite element model which has been calibrated and validated against experimental data in Daiyan et al. (2010b) is used for numerical studies in this paper.

2 NUMERICAL MODELING

The numerical model to simulate pipeline/soil interaction was developed using the finite element software package ABAQUS/Standard. A three-dimensional continuum model (Figure 1) has been developed and validated using centrifuge tests data (Daiyan et al. 2010b). Dimensions of the modeled soil domain were selected to minimize boundary effects on the predicted soil load, displacement and failure mechanisms.

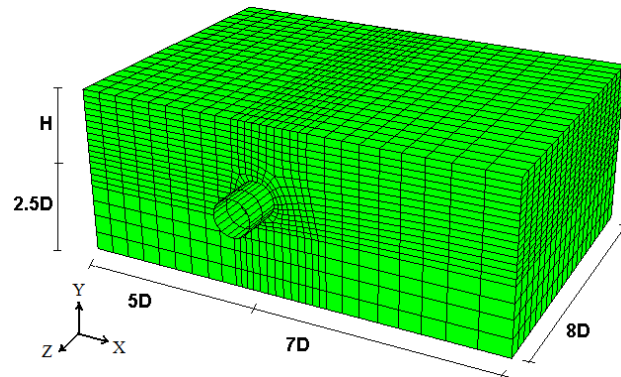


Figure 1: The finite element model geometry

Linear eight node brick elements with reduced integration (C3D8R) for soil and four node shell elements (S4R5) for pipe are used. The interface between pipe and soil is simulated using the contact surface approach implemented in ABAQUS/Standard. This approach allows for separation and sliding of finite amplitude and arbitrary rotation of the contact surfaces. The Coulomb friction

model is used for the frictional interface between pipe and dry sand. In this method, the friction coefficient is defined as $\mu = \tan(\delta)$, where δ is the pipe/soil interface friction angle. Sliding occurs after the shear stress on the contact surface exceeds the critical shear stress. The critical shear stress is the product of μ and contact pressure.

As the main purpose of the study was the load-displacement relationship in the soil, a rigid pipe is used during the analysis. In the numerical model the pipe displacement is applied to all nodes of the pipe to simulate a rigid pipe. To minimize end effects of soil boundaries on the pipe, only the central region having uniform stress conditions was examined. About one-third of the pipe length at the middle was considered to calculate the soil load on the unit length of the pipe.

The numerical analysis is conducted in two main steps. The first step is a geostatic stress step that accounts for the effects of pipe and soil weight to determine the initial stress state in the soil. The second step is to impose the pipe displacement in the specified direction (i.e. oblique angle).

The soil elastic modulus is defined using the following relation to simulate its dependence on effective confining pressure, p :

$$E = E_0 \left(\frac{p}{p_0} \right)^n \quad [2]$$

In Eq. 2, p_0 is a reference pressure equal to the atmospheric pressure ($p_0 = 100$ kPa), E_0 is the soil elastic modulus at the reference pressure and n is the power exponent ($n = 0.5$). The elastic modulus at the reference pressure ($E_0 = 15000$ kPa) was calibrated against the triaxial test data. The Poisson's ratio was assumed to be 0.3. A minimum value of cohesion of 4 kPa was necessary for numerical convergence in pipe/soil interaction model.

The non-associated Mohr-Coulomb plasticity model implemented in ABAQUS/Standard is used to simulate the sand behaviour. Such Mohr-Coulomb models have been successfully used for several studies on pipe/soil interaction involving large soil deformations such as Popescu et al. (2002), Yimsiri et al. (2004).

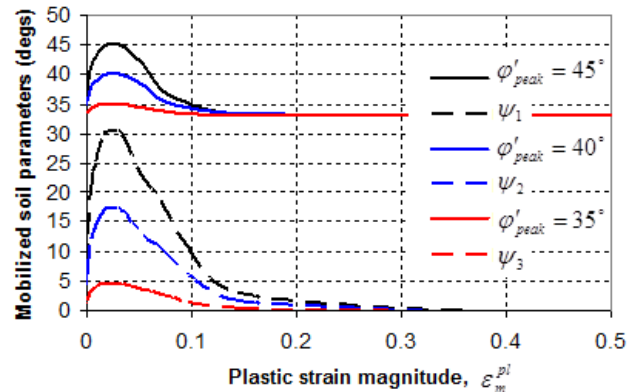


Figure 2: Mobilization of friction and dilation angles used for parametric studies. ψ_1 , ψ_2 and ψ_3 are dilation angles relevant to peak friction angles of 45, 40 and 35 degrees respectively.

Dense sand exhibits a strain hardening and softening response with shear induced dilative behavior. To estimate the progressive mobilization of soil shear strength parameters, the internal friction angle and dilation angle of sand are defined as a function of plastic strain magnitude as a state parameter. The calibration procedure using triaxial data is discussed in detail in Daiyan et al. (2010b).

The progressive mobilization of soil strength parameters for three different peak friction angles of sand investigated in this study ($\phi_{peak} = 35, 40$ and 45°) are presented in Figure 2. These functions are implemented in the finite element simulation through a user subroutine. Constant volume friction angle (ϕ_{cv}) of the silica sand investigated in this study is equal to 33° .

3 AXIAL-VERTICAL PIPE/SOIL INTERACTION

3.1 Review of Previous Studies

As mentioned earlier, the authors could not find any study on the axial-vertical pipe/soil interaction in the literature. A numerical study on pipe/soil interaction in clay by Phillips et al. (2004) and experimental (Daiyan et al. 21010a) and numerical (Daiyan et al. 2010b) studies by the authors on sand, have shown the axial-lateral pipe/soil interaction can be represented schematically as Figure 3. The interaction curve has two parts. The linear part represents the increase in axial restraint on the pipeline by imposing a lateral load. The curved part shows a change in mechanism from failure on pipe/soil interface to shear failure in the soil. The following equation is proposed for the curved part:

$$N_{qh}^2 + 3N_t^2 = N_{qh(90)}^2 \quad [3]$$

The lateral interaction factor is defined as:

$$N_{qh} = \frac{P_u}{\gamma' HD} \quad [4]$$

where P_u is the ultimate lateral load on pipe (P is the lateral load applied to the unit length of the pipeline). In Eq. 3, $N_{qh(90)}$ is the ultimate lateral interaction factor during pure lateral pipe/soil relative movement. In Eq. 4, γ' is soil unit weight, H is the burial depth to the pipe centerline and D is the outer diameter of pipe. The axial interaction factor is defined as:

$$N_t = \frac{T_u}{\gamma' HD} \quad [5]$$

where T_u is the ultimate axial load per unit length of the pipeline.

The linear part in Figure 3 connects the point associated with the pure axial condition to a point with

horizontal coordinate of $(\mu \cdot N_{qh})$ and vertical coordinate of (N_{qh}) .

3.2 Results and Discussions

This paper uses a similar procedure with the validated numerical model to investigate the pipe/soil interaction in axial-vertical (upward) oblique plane.

Figure 4 compares the load-displacement curves for vertical upward movement of pipe with different burial depths, friction angles and pipe surface friction factors ($f = \delta/\phi$).

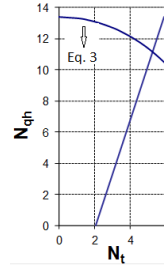


Figure 3: Interaction curve for axial-lateral pipe/soil interaction.

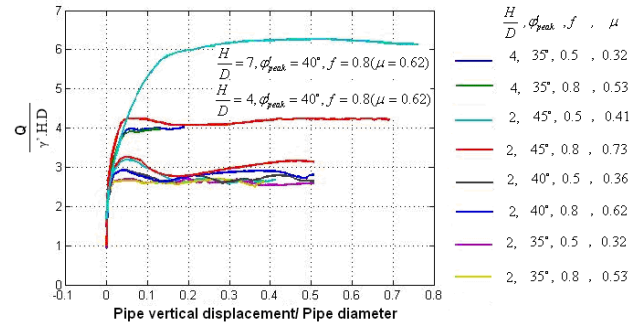


Figure 4: Vertical uplift load-displacement curves

The ultimate vertical loads, which are chosen as peak loads from Figure 4, compare well with rigorous finite element limit analysis by Merifield and Sloan (2006) for horizontal anchor plates. It is well known that the vertical soil restraint on the pipeline increases by increasing the burial depth and reaches a maximum in a critical depth where a flow around mechanism (deep mechanism) occurs. Previous studies (e.g. Yimsiri et al 2004) have shown the deep mechanism occurs at burial depths $H/D > 21$ for the range of soil shear strength parameters in this study. Therefore in the current study with a range of burial depths less than 7 ($H/D \leq 7$) this deep mechanism was not observed.

Increasing the soil peak friction angle increases the vertical soil restraint on the pipeline. Figure 4 shows pipe surface roughness has no or little effect on the ultimate vertical load on the pipeline which is consistent with previous studies e.g. Rowe and Davis (1982) and Merifield and Sloan (2006), however pipe surface roughness affects the load on the pipeline at large displacements ($> 0.2D$). For smooth pipelines load-displacement curves for different friction angles converge to residual state at large displacements, but when the

pipeline surface is rough the load on the pipeline increases at large displacements depending on the soil friction angle.

A comparison of displacement fields in the soil during upward movement of pipe are presented in Figure 5 for a pipe displacement (d) of $0.15D$, where the load-displacement curves reach a residual state. The displacement fields include a rigid column of soil immediately above the pipe that moves upward, and a plastic zone of lateral and upward movement at the two sides of the rigid column of soil which is consistent with what is shown for horizontal anchor plates by Merifield and Sloan (2006). The size of this curved plastic zone is affected by soil friction angle and dilatancy, as is expected based on e.g. Rowe (1978) and Cheuk et al. (2008) among others.

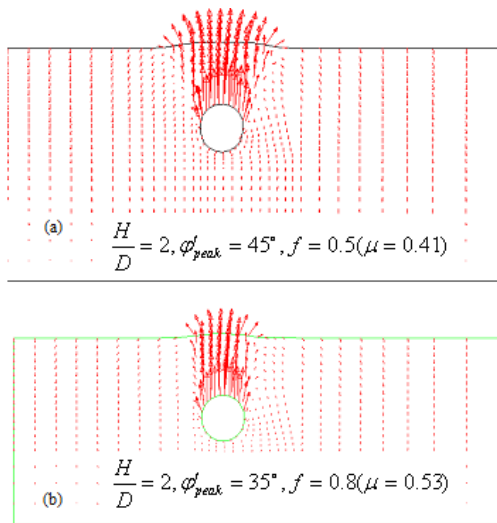


Figure 5: Comparison of displacement fields in soil for different friction angles ($H/D=2$, $d=0.15D$).

Numerical axial-vertical pipe/soil interaction analyses are conducted for various parameters. Unit weight of soil is assumed constant equal to 16 kN/m^3 for all cases. To determine the pipe selfweight, a steel pipe with diameter over thickness ratio of $D/t \approx 50$ is assumed. Pipe selfweight makes a small fraction of the vertical interaction factor. For example for a burial depth ratio of $H/D=2$, $D=0.5 \text{ m}$ and pipe selfweight $W_p=118 \text{ kg/m}$, the contribution of pipe selfweight to the vertical interaction factor is $W_p/\gamma \cdot H \cdot D = 0.145$ which is about 6% of the total vertical interaction factor. As shown by Cheuk et al. (2008), the vertical resistance mainly comprises of geostatic vertical stress and shearing resistance.

Axial and vertical load-displacement curves for different oblique angles (Figure 6) for the case of a pipe buried at a burial depth of $H/D=4$, in a sand with $\phi_{peak}=40^\circ$ and pipe surface friction factor $f=0.8$ ($\mu=0.62$), are presented in Figure 7.

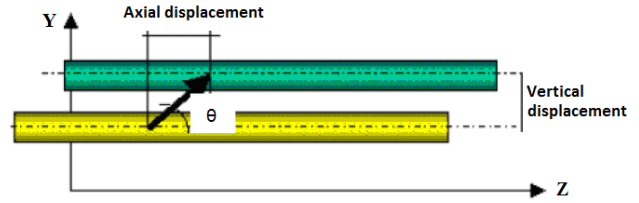


Figure 6: Axial-vertical oblique angle.

The definition of oblique angle is shown in Figure 6 where θ is equal to 0° for pure axial and 90° for vertical upward movements.

In Figure 7, T and Q are the same as defined in Eq. 1. As shown in Figure 7, an interaction effect similar to what was reported during axial-lateral pipe/soil interaction (Daiyan et al. 2010b) happens during axial-vertical relative movement between pipeline and soil. The ultimate axial load on the pipeline increases by about 50% with respect to pure axial movement for small oblique angles. This increase is lower than what was observed during axial-lateral pipe/soil interaction which can be attributed to the fact that vertical soil restraint on the pipe is lower than lateral restraint, therefore the increase in normal load on the pipe surface during axial-vertical pipe/soil interaction is lower.

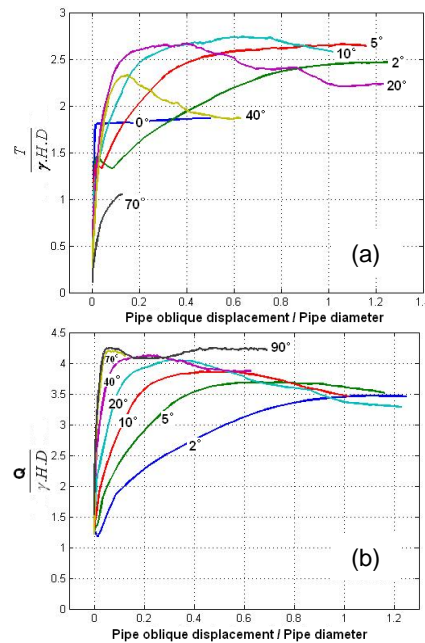


Figure 7: Axial (a) and vertical (b) load-displacement curves for different oblique angles; $H/D=4$, $\phi_{peak}=40^\circ$, $f=0.8$ ($\mu=0.62$).

For small oblique angles (2° and 5° in Figure 7), at early stages of loading, the axial load on the pipeline decreases and then increases again at larger relative displacements. Figure 8 shows how the axial load on the pipe circumference changes during various increments of oblique 2° axial-vertical movement. In Figure 8.b, T_n is the axial load applied to each node on the pipe circumference. The axial load on the pipe is increasing from increment 1 to increment 7 as the axial resistance on the pipe surface is being mobilized by a small axial displacement. Pipe

displacement relevant to each increment can be found in Figure 8.a. From increment 7 to 13 the axial load on the pipe decreases because of the gap occurring at the bottom of the pipe as a result of upward movement of the pipe. For the rest of oblique displacement increments, the peripheral area of the pipe in contact with soil remains constant and almost half of the circumference is involved in pipe/soil interaction. The axial load on the pipe increases by increasing the vertical component of the load (Figure 8.a) and, as a result, the normal pressure on the pipe surface.

Axial and vertical interaction factors for different parameters are compared in Figure 9, 10 and 11. Similar to axial-lateral pipe/soil interaction a two part interaction curve seems to fit to all data sets well. The equations are different from what was proposed for axial-lateral pipe/soil interaction (Eq. 3) and consist of a linear part that connects the point $(N_{t(0)}, 0)$ and $(\mu \cdot (N_{qv(90)} + 0.7), N_{qv(90)})$, and a curve part with the following equation:

$$N_{qv}^2 + 0.3N_t^2 = N_{qv(90)}^2 \quad [6]$$

where $N_{qv(90)}$ is interaction factor for pure vertical loading condition. The vertical interaction factor is defined as:

$$N_{qv} = \frac{Q_u}{\gamma_c H D} \quad [7]$$

where Q_u is the ultimate vertical component of the load per unit length of the pipeline.

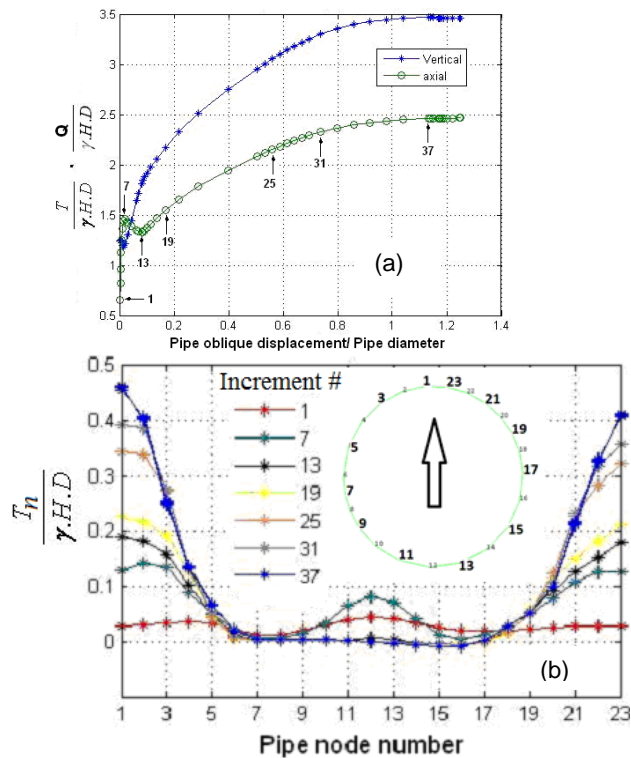


Figure 8: (a) Axial-vertical load-displacement curves for oblique 2°, and (b) normalized axial loads applied at different nodes of the pipe at specified increments shown in (a).

Figure 9 shows the effect of soil friction angle on axial and vertical components of load on the pipeline. By increasing the friction angle the failure surface expands and both axial and vertical components of load increase accordingly.

The effect of the roughness of the pipe external coating on axial-vertical interaction curves is shown in Figure 10. Two different friction factors (f) of 0.5 and 0.8 are used resembling pipelines with smooth (e.g. polyethylene) and rough (e.g. steel) external surfaces respectively. For constant soil parameters and geometrical conditions increasing the pipe surface friction factor from 0.5 to 0.8 increases the axial load on pipeline for oblique angles lower than or equal to 40°. Increasing the axial component of load on pipeline decreases the vertical component of the load according to Eq. 6. For higher oblique angles the surface roughness has little or no effect on the soil restraint on the pipe. The pure vertical interaction factor ($N_{qv(90)}$) does not change by increasing the roughness of pipe external surface.

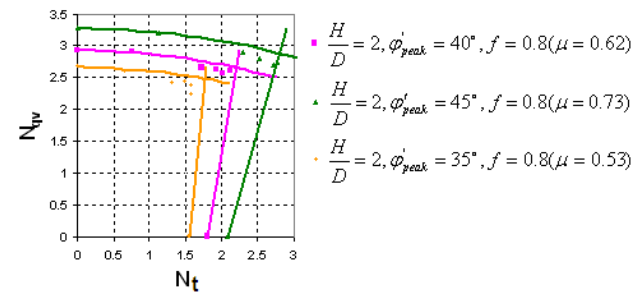


Figure 9: Effect of friction angle on axial-vertical pipe/soil interaction

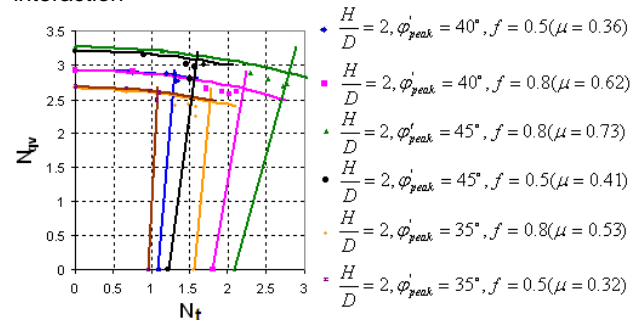


Figure 10: Effect of interface friction factor on axial-vertical pipe/soil interaction

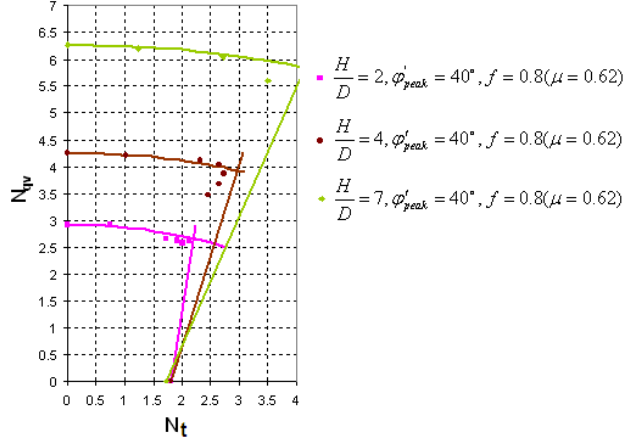


Figure 11: Effect of burial depth on axial-vertical pipe/soil interaction.

The effect of burial depth ratio is shown in Figure 11. By increasing the burial depth the vertical load on the pipe increases which results in larger normal stress on the pipe surface and increases the axial load on the pipeline.

4 LATERAL-VERTICAL PIPE/SOIL INTERACTION

4.1 Review of Previous Studies

There are several studies that have investigated the loads and displacements in lateral and vertical directions on pipelines (e.g. Trautmann 1983, Yimsiri et al. 2004) and also oblique lateral-vertical pipe/soil interactions (e.g. Hsu 1996, Calvetti et al. 2004).

Nyman (1984) performed an implicit limit equilibrium analysis on pipes buried in cohesionless soils based on limit equilibrium model for inclined anchor plates. Nyman used a failure mechanism including a passive wedge with planar failure surfaces which is acceptable for shallow burial depths. The ultimate soil restraint in the oblique direction is presented as:

$$P_{u-oblique} = iQ_u \quad [8]$$

where:

$$i = 1 + \frac{\hat{e}}{\hat{e}_{90^\circ}} \frac{0.25a\hat{c}}{0.75a\hat{c}} \frac{\hat{u}}{\hat{h}} (i_u - 1) \quad [9]$$

$i_u = P_u / Q_u$ is the ratio of ultimate lateral (horizontal) restraint to ultimate vertical restraint and α' is shown in Figure 12.

Nyman proposed the ultimate oblique displacement as 0.015H to 0.025H for dense to loose materials, respectively.

Experimental results by Das (1985) from small scale tests on anchor plates in clay and by Hsu (1996) from large scale tests on pipes in loose sand indicate good agreement with Eq. 8. They have also shown that the oblique (lateral-vertical) restraint does not change greatly

for α' from zero to 45 and most of increase happens for α' from 45 to 90°.

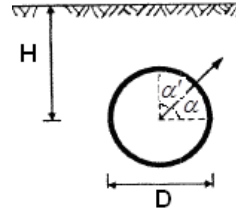


Figure 12: Oblique angle in lateral-vertical plane.

Several researchers analysed the lateral-vertical pipeline/soil interaction using a plasticity model. These models consist of a failure locus or interaction curve which relates the lateral and vertical ultimate loads and an associated (e.g. Guo 2005) or non-associated (e.g. Calvetti et al. 2004) flow rule to determine the plastic displacement increments. Failure loci from some studies are discussed here.

Guo (2005) developed an associative hardening elastoplastic constitutive model for lateral-vertical upward pipe/soil interaction in clay. A circular relationship between normalized lateral and vertical loads (by pure lateral and pure vertical soil restraints) was used as failure locus. He indicated good agreement between his model's predictions and his numerical model's results as well as Hsu's (1996) experimental results.

Zhang et al. (2002) presented a yield surface along with a plasticity model for lateral-vertical pipe/soil interaction for shallow buried (or half-buried) pipelines in sand (sea bed).

Hodder and Cassidy (2010) presented a similar study on developing a plasticity model for lateral-vertical interaction of soil with shallow buried pipes in clay.

Cocchetti et al. (2009a) proposed a 3D failure criterion for pipelines buried in sand, but they assumed no interaction in axial-lateral and axial-vertical planes. Their proposed failure criterion in lateral-vertical plane is compared with other researchers in next section.

Cocchetti et al. (2009a & 2009b) also proposed an improved spring model for structural analysis of pipe/soil interaction events.

4.2 Results and Discussions

The same numerical model that was used for parametric studies in previous sections is used for lateral-vertical pipe/soil interaction.

Load/displacement curves for two different cases are presented in Figures 13 and 14. The oblique angles α in lateral-vertical plane are shown in Figure 12 where for pure lateral movement $\alpha = 0^\circ$ and for vertical upward movement $\alpha = 90^\circ$.

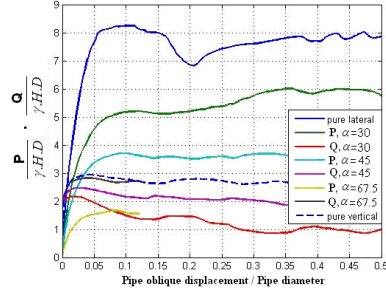


Figure 13: Lateral-vertical load-displacement curves for $H/D=2$, $\phi=40^\circ$, $f=0.5$.

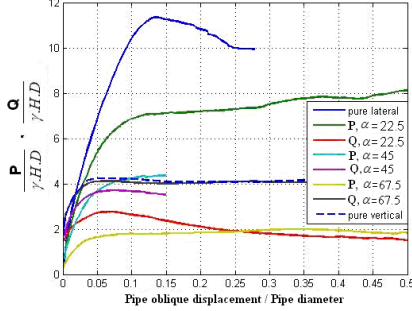


Figure 14: Lateral-vertical load-displacement curves for $H/D=4$, $\phi=40^\circ$, $f=0.8$.

The load-displacement curves show that the effect of oblique movement is more significant for lateral component of the load on the pipeline as the range of difference in vertical load is much less than lateral load. For instance an obliquity of equal to or less than 22.5° with respect to vertical direction has almost no effect on vertical component of load on the pipe.

Interaction factors presented in Figure 15 are normalized by pure lateral and pure vertical upward interaction factors. The yield surface is part of a circle:

$$\frac{\frac{P}{\gamma H D}}{\frac{P}{\gamma H D(0)}}^2 + \frac{\frac{Q}{\gamma H D}}{\frac{Q}{\gamma H D(90)}}^2 = 1 \quad [10]$$

Guo (2005) presented a similar yield surface for lateral-vertical upward pipe/soil interaction in clay. Figure 15 shows numerical data points are scattered around this yield surface.

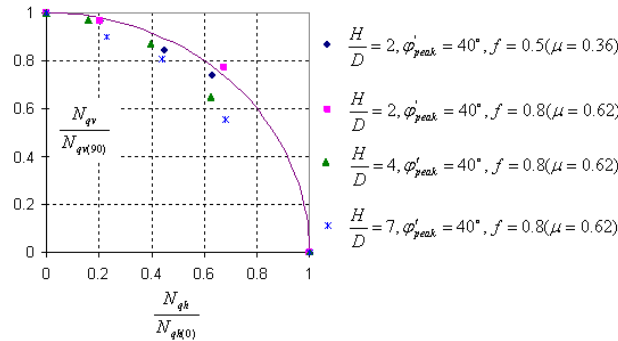


Figure 15: Summary of normalized interaction factors for lateral-vertical upward pipe/soil interaction.

Figure 16 compares the continuum finite element results with Nyman (1984) theoretical interaction curve. Numerical data points show very good agreement with Nyman's interaction curve. A few data points related to $H/D=2$ are a bit away from the interaction curve which is probably because of Nyman's assumption that the direction of pipe movement in the soil coincides with the direction of resultant load on the pipeline. Figure 17 shows this assumption is correct for deeply buried pipes while it is not correct for the case of oblique movement of shallow buried pipes.

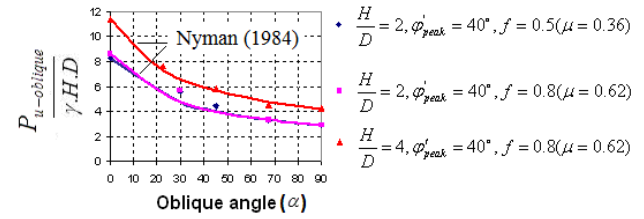


Figure 16: Comparison of FE data points with Nyman's interaction curve.

Figure 18 shows a comparison of yield surfaces suggested by other studies with the numerical finite element data from current study for one set of parameters. Numerical data show very good match with the yield surface suggested by Cochetti et al. (2009a). Failure surfaces proposed by Zhang et al. (2002) and Hodder and Cassidy (2010) for half buried pipelines are consistent.

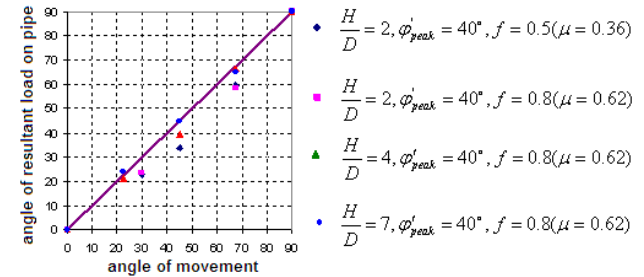


Figure 17: Direction of oblique load vs. oblique movement during lateral-vertical upward pipe/soil interaction.

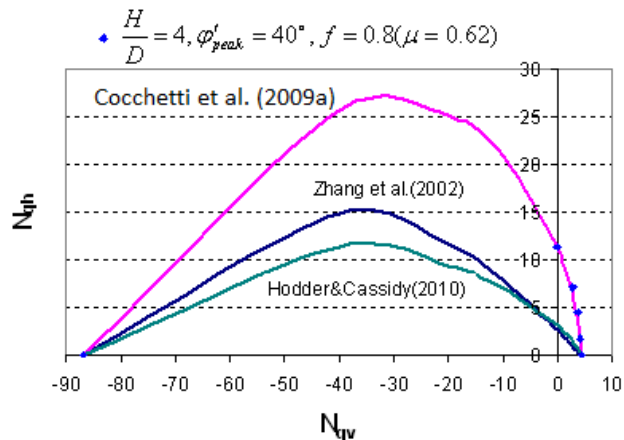


Figure 18: Comparison of various yield surfaces with numerical data from this study for lateral-vertical pipe/soil interaction (vertical upward +, vertical downward -).

For buried pipelines the failure surface proposed by Cocchetti et al. (2009a) can be adopted for lateral-vertical (upward/downward) pipe/soil interaction. Combining this equation with axial-lateral and axial-vertical interaction curves gives a 3D yield surface for pipe/soil interaction problems.

Numerical studies by Cocchetti et al. (2009a) and Calvetti et al. (2004) show a considerable interaction between lateral and vertical downward soil restraints on the pipe. As indicated in Figure 18, the lateral soil restraint on the pipeline may increase dramatically when downward relative displacement between pipe and soil exists. This interaction effect is not considered in the current guidelines as well.

5 CONCLUSIONS

Numerical investigation using finite element software ABAQUS in this paper have shown the significance of load coupling mechanisms during axial-vertical (upward) pipe-soil interaction. The axial load is shown to increase by about 50% during axial-vertical movement while the vertical component of the load on the pipeline decreases slightly for small oblique angles.

A two-part failure criterion is proposed for oblique axial-vertical pipeline/soil interaction. The failure criterion is based on the same concept as the axial-lateral failure surface which was published by the authors. The failure criterion includes a linear part that defines soil failure mechanism on the pipeline circumference for low oblique angles, and a curved part that explains shear failure mechanisms through the soil at higher oblique angles of movement.

Parametric studies are conducted to investigate the effect of soil friction angle, pipe/soil interface friction factor and pipe burial depth on axial-vertical pipeline/soil interaction. The proposed failure criterion fits well numerical data from various sets of parameters well.

Numerical analyses are conducted to investigate lateral-vertical (upward) pipe/soil interaction. The numerical simulations were consistent with failure criteria

proposed by Nyman (1984) and Cocchetti et al. (2009a). Cocchetti et al. (2009a) criteria show a significant interaction between lateral and vertical loads on the pipeline during lateral-vertical (downward pipe/soil interaction which is not accounted for in the current guidelines.

These observations show the current guidelines based on structural pipeline/soil interaction models need to be improved to be able to account for a 3D pipe/soil relative movement. Adding the axial-lateral and axial-vertical pipe/soil interaction effects to Cocchetti et al. (2009a) can provide a reliable tool to conduct pipe/soil interaction structural modeling using enhanced spring models such as Cocchetti et al. (2009b).

REFERENCES

- ALA (2001). Guidelines for the design of buried steel pipe, American Lifeline Alliance, www.americanlifelinealliance.org
- Calvetti, F., Prisco, C., and Nova, R. (2004). Experimental and numerical analysis of soil-pipe interaction. *Journal of Geotechnical and Geoenvironmental Engineering*, Vol. 130, No. 12.
- Cheuk, C. Y., White, D. J., Bolton, M. D. (2008). Uplift mechanisms of pipes buried in sand. *Journal of Geotechnical and Geoenvironmental Engineering*, ASCE, 134(2).
- Cocchetti, G., Prisco, C., Galli, A. and Nova, R. (2009a). "Soil-pipeline interaction along unstable slopes: a coupled three-dimensional approach. Part 1: Theoretical formulation." *Can. Geotech. J.* 46: 1289-1304.
- Cocchetti, G., Prisco, C., Galli, A. (2009b). "Soil-pipeline interaction along unstable slopes: a coupled three-dimensional approach. Part 2: Numerical analyses". *Can. Geotech. J.* 46: 1305-1321.
- Daiyan, N., Kenny, S., Phillips, R. and Popescu, R. (2010a). "Investigation of axial/lateral interaction of pipes in dense sand." ICPMG 2010, Int. Conf. on Physical Modeling in Geotechnics, Zurich, Switzerland.
- Daiyan, N., Kenny, S., Phillips, R. and Popescu, R. (2010b). "Numerical investigation of oblique pipeline/soil interaction in sand." IPC 2010, Int. Pipeline Conf., Calgary, Canada.
- Das, B. M. (1985). Resistance of shallow inclined anchors in clay. Uplift behavior of anchor foundations in soil, S.P. Clemence, ed., ASCE, New York.
- Guo, P. (2005). Numerical modeling of pipe-soil interaction under oblique loading. *Journal of Geotechnical and Geoenvironmental Engineering*, ASCE, 131(2), pp. 260- 268.
- Hodder, M. S. and Cassidy, M. J. (2010). A plasticity model for predicting the vertical and lateral behavior of pipelines in clay soils. *Geotechnique*, 60, No. 4, pp. 247-263.
- Honegger, D.G., Nyman, J. (2004). "Guidelines for the seismic design and assessment of natural gas and liquid hydrocarbon." Pipeline Research Council International Project PR-268-9823.

- Hsu, T. W. (1996). Soil restraint against oblique motion of pipelines in sand. *Canadian Geotechnical Journal*, pp. 180-188.
- Merifield, R. S. and Sloan, S. W. (2006). The ultimate pullout capacity of anchors in frictional soils. *Canadian Geotechnical Journal*, 43, pp. 852-868.
- Nyman, K.J. (1984). Soil response against oblique motion of pipes. *Journal of Transportation Engineering*, 110(2), pp. 190-202.
- Phillips, R., Nobahar, A. and Zhou, J. (2004). Combined axial and lateral pipe-soil interaction relationships. Proceedings of IPC2004, international pipeline conference, Calgary, Canada.
- Popescu, R., Phillips, R., Konuk, I., Guo, P., and Nobahar, A. (2002). Pipe-soil interaction: Large-scale tests and numerical modeling. Proceedings of International Conference on Physical Modeling in Geotechnics, ICPMG'02, St. John's, Newfoundland, pp. 917-922.
- Rowe, R. K. (1978). Soil structure interaction analysis and its application to the prediction of anchor behaviour. Ph.D. thesis, University of Sydney, Sydney, Australia.
- Rowe, R. K., and Davis, E. H. (1982). The behavior of anchor plates in sand. *Geotechnique*, 32(1), pp. 25-41.
- Trautmann, C. H. (1983). Behavior of pipe in dry sand under lateral and uplift loading. Ph.D. thesis, Cornell University, Ithaca, New York.
- Yimsiri, S., Soga, K., Yoshizaki, K., Dasari, G. R. and O'Rourke, T. D. (2004) Lateral and upward soil-pipeline interactions in sand for deep embedment conditions. *Journal of Geotechnical and Geoenvironmental Engineering*, 130(8), pp. 830-842.
- Zhang, J., Stewart, D. P. and Randolph, M. F. (2002). Modeling of shallowly embedded offshore pipelines in calcareous sand. *Journal of Geotechnical and Geoenvironmental Engineering*. ASCE, Vol. 128, No.5, pp. 363-371.